

8-Element Wide-Beam Circular Bond-Wire Array Antenna for 60 GHz Wireless Communication

R. van Kemenade*, C. Jarufe†, R. Finger‡, A.B. Smolders* and L. Bronfman‡

* Eindhoven University of Technology, Department of Electrical Engineering, Eindhoven, The Netherlands

† University of Chile, Department of Electrical Engineering, Santiago, Chile

‡ University of Chile, Department of Astronomy, Santiago, Chile

E-mail: rfinger@das.uchile.cl

Abstract—Bond-wire antennas (BWAs) are an attractive concept for integrated radio front-ends at millimetre-wave frequencies, but have a relatively narrow radiation pattern that makes them less attractive for many applications. In this paper, a circular BWA array antenna concept is presented that has a broad and omnidirectional radiation pattern. The relationship between array geometry and the shape of the gain pattern has been extensively explored through a series of parametric simulations. A prototype was built and measured in order to verify simulation results. The main suggested cause for a difference between simulated and measured data are inaccuracies in the design and manufacturing process of the feed network.

I. INTRODUCTION

An ever-continuing trend in the area of (tele)communication technology is the pursuit of higher data transfer rates. For short range wireless communication purposes such as Wi-Fi and point-to-point networks, the 60 GHz Industrial, Scientific and Medical (ISM) band provides 7 GHz of license-free bandwidth in most parts of the world. This band is thus gaining popularity for its enormous application potential [1]. With shorter wavelengths, antennas can also be made much smaller, which is leading to new antenna designs that can be fully integrated with the front-end electronics. The two types of integrated antenna concepts that have received most attention are the Antenna on Chip (AoC) and the Antenna in Package (AiP) [2]. A third, hybrid, antenna model is the Bond-Wire Antenna (BWA) [3], which combines a relatively high radiation efficiency with excellent integration possibilities. It comprises of a bond-wire that is placed in a semi-circular arc shape above a (reflecting) ground plane. It does not require an extra transmission line between the front-end and the antenna and furthermore, the BWA can be very easily manufactured using equipment already widely available to chip manufacturers, which makes it a low-cost option.

The free-space signal attenuation is very high at 60 GHz (68 dB at a 1 m distance). Thus, in a wireless communication system, the combined antenna gain between receiver and transmitter will need to be high in order to have a sufficient carrier-to-noise ratio. For example, in order to achieve a 2 Gbps data rate with QPSK modulation in a 10 m line-of-sight (LOS) situation, a combined antenna gain of 33 dBi is required [2]. Therefore, it makes sense that much research is done into making integrated antennas directive. For a Wi-Fi access point type application, however, an antenna with a

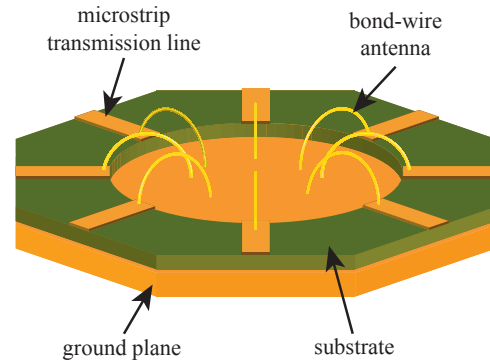


Fig. 1: Artist's impression of a MS-fed circular BWA array.

broad radiation pattern is much more practical. A suggested option is to use a directive antenna at the connecting client's side (for example, a phased array with active beam steering embedded in a mobile device) and an antenna with a broader radiation pattern at the access point. An extensive study on the feasibility of such communication channels was done in [4].

In this paper we propose a circular BWA array concept, as is shown in Fig. 1, with an omnidirectional radiation pattern that can be used as a non-directive access point antenna for 60 GHz wireless communication. In Section II, the design is introduced. A prototype was manufactured and measured as described in Sections III, with measurement results and analysis in Section IV. Conclusions and recommendations for future work are given in Section V.

II. ARRAY ANTENNA DESIGN

A. Bond-Wire Antennas

The BWA is introduced in [3], where wire length is $\frac{\lambda_0}{2}$. For an antenna that operates at 60 GHz, this means that a wire length of $l = 2.5$ mm should be used, which corresponds to a half-loop with a radius of $b \approx 0.8$ mm. A prototype was successfully demonstrated at 40 GHz in [5], including a study of the influence of the size of the ground plane.

A single BWA in combination with a ground plane may be considered an electrically large loop antenna (through image

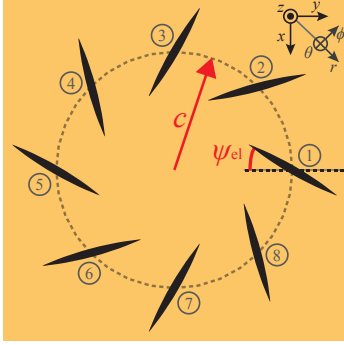


Fig. 2: 8-element BWA array parameters, birds-eye view.

theory). As such, it has a fairly narrow radiation pattern. By placing BWAs in a circular array (concept shown in Fig. 1) we can achieve a radiation pattern that is fairly broad along θ and close to omnidirectional in ϕ .

B. Array Configuration

A circular array introduces many degrees of freedom in the design process. These include the number of elements (N), the array radius (c) and the rotation of each element around its own axis (ψ_{el}). Also, we can change the relative phase of each element's feed port (φ_{src}). The geometrical parameters c and ψ_{el} for an 8-element array are indicated in Fig. 2, where the angle ψ_{el} is the same for each element. Varying these parameters has consequences for the total radiation pattern. Obtaining the right radiation characteristics therefore takes some tuning of the design.

C. Tuning the Design

We will characterize our radiation pattern by means of its angle of maximum gain (θ_{max}), the value of this maximum gain (G_{max}) and the half-power beamwidth (HPBW), each with respect to θ (definitions from [6]). Relationships between the radiation pattern and the array geometry were obtained from parametric simulations in Ansoft HFSS [7].

Simulations were performed in the form of parametric sweeps over the geometric variables described in II-B as well as the relative phase of the antenna element ports φ_{src} . The data were then studied to analyze the consequences for the radiation pattern. In general, we may state that the radiation pattern becomes more omnidirectional as we increase the number of elements. As a compromise between manufacturing feasibility and omnidirectionality, we choose to fix the number of elements at $N = 8$. Furthermore, we see that varying the element angle ψ_{el} has minimal influence on the radiation pattern and thus it was fixed to $\psi_{el} = 0^\circ$, as this architecture is the easiest to manufacture. Fig. 3 shows how the radiation pattern changes for such an array at a fixed relative element port phase $\varphi_{src} = 45^\circ$ for different values of c . Fig. 4 goes on to show how the extracted antenna parameters change for varying c , for three different relative element port phases. In the leftmost two plots, the sudden jump in the $\varphi_{src} = 0^\circ$ line at $c \approx 3.4$ mm occurs due to the second lobe of the radiation

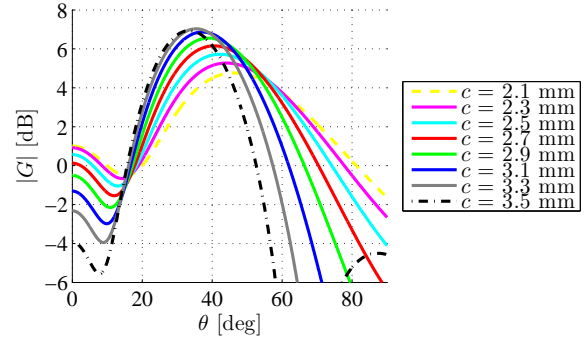


Fig. 3: Antenna gain (E -plane) for $\psi_{el} = 0^\circ$, port phase $\varphi_{src} = 45^\circ$ and a varying array radius c .

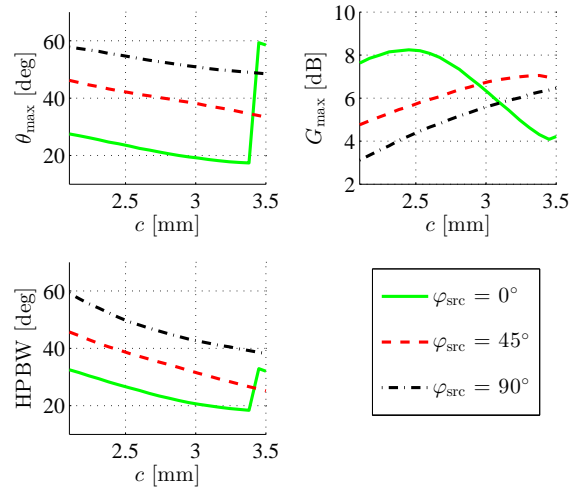


Fig. 4: Angle of maximum directivity, value of maximum directivity and HPBW for varying c at three different values of φ_{src} .

pattern becoming dominant. The polarization of the far field is vertically linear; similar to that of an infinitesimal z -oriented electric dipole at the center of the array.

III. PROTOTYPE

In order to verify the simulation results, a prototype BWA array with a radius of $c = 2.5$ mm was designed and manufactured to perform at 60 GHz. The relative excitation port phase was chosen to be $\varphi_{src} = 45^\circ$.

The feed network was designed in Agilent ADS [8] and manufactured using Rogers Duroid 6002 substrate [9] with a thickness of $254 \mu\text{m}$ and a conductor thickness of $35 \mu\text{m}$. Transmission lines were made using a high precision CNC milling machine and the substrate was glued onto a brass ground plane. The BWA array elements were made of AW-14 wire with a $25 \mu\text{m}$ radius and were placed using an industry standard bonding machine. The complete prototype is shown in Fig. 5.

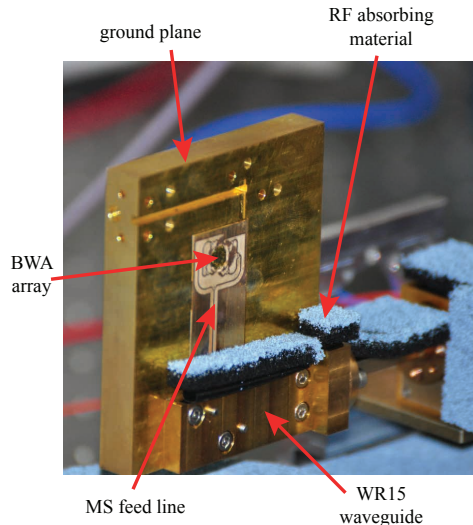


Fig. 5: Photograph of the manufactured prototype structure.

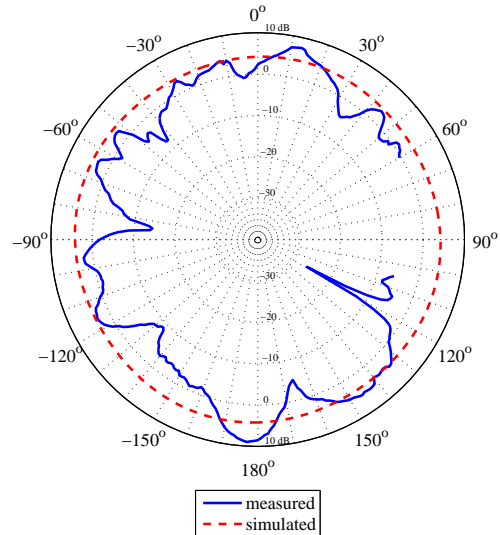


Fig. 7: H -plane slice of the gain pattern of the prototype, measured at $\theta = 30^\circ$.

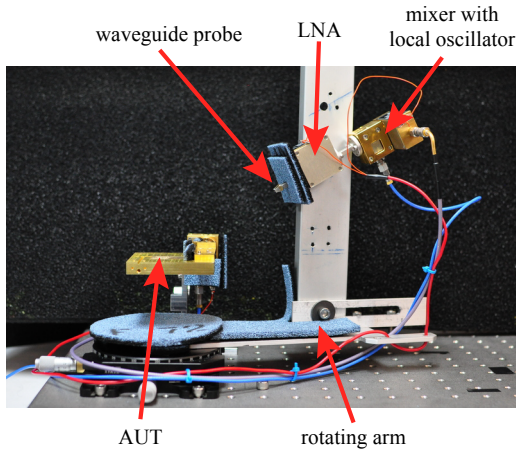


Fig. 6: Array antenna mounted on the radiation pattern measurement setup during an H -plane measurement.

IV. ANTENNA MEASUREMENTS

Measurements were performed in the far field of the array antenna, i.e. for an observation distance $R > \frac{2D^2}{\lambda_0} = 10$ mm, with $D \approx 5$ mm the largest dimension of the array. Nearby surfaces were covered in an RF-absorbing material. The measurement setup is depicted in Fig. 6.

The H -plane slice of the radiation pattern is shown in Fig. 7, in comparison to simulation results. In the figure, there is a missing section in the measured values. This is due to the fact that the measurement probe could not reach those angles in the employed measurement setup. The polarization matches that of the simulation data. Overall, the results show that there are similarities between the measured and simulated data. The deviation is, however, too large to speak of a good match. Two causes are suggested.

The first suggested cause of deviation in the radiation pattern is an inevitable difference in the wire length. Placing the

elements by hand using a standard bonding machine introduces an inaccuracy that has consequences for the resonant frequency of the antenna elements. This has implications in an array configuration, as even a small variation in the wire length can have consequences for the amount of radiated power per element when all elements are working at the same frequency. An analysis in [10] predicts that the manufacturing yield of single BWAs in mass production at 60 GHz with a resonance frequency within a 10% frequency band will be above 99%. In our array configuration, even this relatively small deviation in resonance frequency can potentially cause fluctuations of several dB in the antenna gain for a single element and as such also for the total gain pattern.

Furthermore, it is very likely that there are inaccuracies in the design as well as the manufacturing process of the feed network. The transmission line network was designed using Agilent ADS, which does not incorporate errors like rounded edges (caused by the milling process) and other non-idealities that may play a significant role at 60 GHz. Moreover, the milling machine, although very accurate, may introduce other side-effects that can have a parasitic influence. For examples, the edges of the transmission lines were fairly jagged, and thus fringing of the fields may have occurred here. Besides removing the conductive material, the milling process also removed a thin layer of substrate which alters the characteristic impedance. The accumulation of design and manufacturing inaccuracies most probably has had an effect on the matching of the power lines to the antenna elements (and thus the power transfer) and it is also expected that there is a phase error in the signals delivered to the radiators. A complete set of VNA measurements of (sections of) the feed network may provide

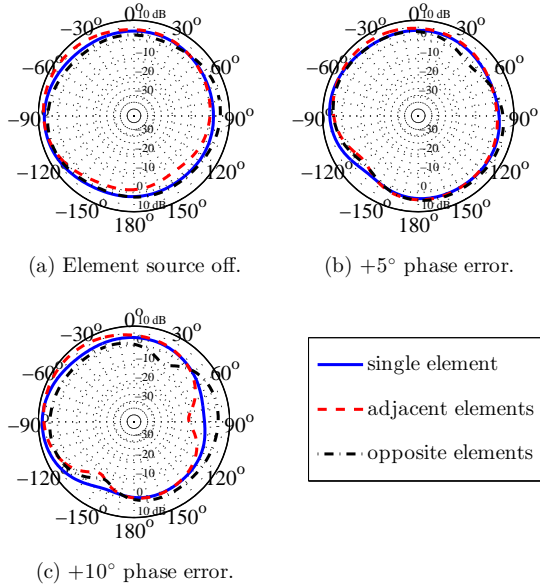


Fig. 8: Simulated gain pattern at $\theta = 30^\circ$ for deliberately introduced feed port errors. Port errors were introduced in a single element, in two adjacent elements and in two opposite elements of the array.

answers. Unfortunately, the measurement equipment required for this was not at hand.

In order to identify the most likely cause of error in the radiation pattern, extra 3D simulations were performed in which deliberate errors were introduced into the feed ports of the array elements. Two types of errors were introduced:

- One or more elements do not receive any power.
- One or more elements have an error in the port phase.

For each case, a situation was considered in which the same error occurred for one element, for two adjacent elements and for two opposite elements in the array. The simulation results are shown in Fig. 8. The phase errors that were introduced are $+5^\circ$ and $+10^\circ$. In Fig 8a we can see that disabling one or two antenna elements does not have large implications for the shape of the gain pattern in the $\theta = 30^\circ$ slice. However, if we look at the effects of a phase error in Fig 8b and Fig. 8c, we can see that if more than one element has a significant phase error, there are also large consequences for the shape of the radiation pattern in the $\theta = 30^\circ$ plane. Considering that drastic improvements can still be made to the design and manufacturing processes of the prototype's feed network we identify phase errors in the feed network (for possibly all ports) to be the most likely cause of the discrepancy between the measured and simulated radiation patterns.

V. CONCLUSIONS AND FUTURE WORK

A circular array concept for integrated bond-wire antennas was presented with a broad and omnidirectional radiation pattern. Through a series of parametric simulations, trends were

studied that relate the geometry and relative array element excitation phase to parameters in the radiation pattern. A prototype was manufactured and measurements were performed. The manufacturing inaccuracy of the antenna feed network is suggested to be the main cause for a difference between measured and simulated radiation patterns. A variation in the targeted antenna element phase can cause a major fluctuation in the radiated power in a certain direction, as was demonstrated with an extra set of simulations.

Future work will include improvements to the design and manufacturing process of the feed network in order to minimize its inaccuracies. Plans include the study and manufacturing of a feed network that uses coplanar waveguides, which will provide a more constant ground plane. To make a reliable prototype, other manufacturing processes will need to be explored in order to guarantee a higher accuracy. Furthermore, it is desirable to perform measurements of solely the feed network before the placing of the bond wires, in order to verify its performance. Finally, extra attention needs to be given to the bonding process, to ensure that antenna elements have uniform length.

VI. ACKNOWLEDGMENT

This research was possible thanks to the support of the Center of Astrophysics and Associated Technologies (CATA-Basal), the project ALMA-CONICYT 31120005, and the Building Interdisciplinary Bridges (CPI2) initiative. The authors thank J. Pizarro for manufacturing the prototype and C. Estévez for providing the 60 GHz RF equipment that was used during measurements.

REFERENCES

- [1] P. Smulders, "Exploiting the 60 GHz Band for Local Wireless Multimedia Access: Prospects and Future Directions," *IEEE Communications Magazine*, no. January, pp. 140–147, 2002.
- [2] Y. Zhang and D. Liu, "Antenna-on-Chip and Antenna-in-Package Solutions to Highly Integrated Millimeter-Wave Devices for Wireless Communications," *IEEE Transactions on Antennas and Propagation*, vol. 57, no. 10, pp. 2830–2841, 2009.
- [3] N. Varanasi and D. Peroulis, "On-chip bond-wire antennas on CMOS-grade silicon substrates," in *2008 IEEE Antennas and Propagation Society International Symposium*, no. 1. IEEE, Jul. 2008, pp. 1–4.
- [4] H. Yang, P. Smulders, and M. Herben, "Channel Characteristics and Transmission Performance for Various Channel Configurations at 60 GHz," *EURASIP Journal on Wireless Communications and Networking*, vol. 2007, no. 1, p. 019613, 2007.
- [5] R. Willmot, D. Kim, and D. Peroulis, "High-efficiency wire bond antennas for on-chip radios," in *2009 IEEE MTT-S International Microwave Symposium Digest*. Boston, MA: IEEE, Jun. 2009, pp. 1561–1564.
- [6] C. Balanis, *Antenna Theory: Analysis and Design*, 3rd ed. Hoboken, New Jersey: John Wiley & Sons, Inc., 2005.
- [7] Ansoft, "Ansoft High Frequency Structure Simulator (HFSS) website." [Online]. Available: <http://www.ansys.com/>
- [8] Agilent, "Agilent EEsof Advanced Design System (ADS) website." [Online]. Available: www.home.agilent.com
- [9] Rogers Corporation, "Rogers Corporation website." [Online]. Available: www.rogerscorp.com
- [10] U. Johannsen and A. Smolders, "On the Yield of Millimeter-Wave Bond-Wire-Antennas in High Volume Production," *IEEE Transactions on Antennas and Propagation*, vol. 61, no. 8, pp. 4363–4366, Aug. 2013.